



Exact solutions of Shynaray-IIA equation (S-IIAE) using the improved modified Sardar sub-equation method

Muhammad Ishfaq Khan¹ · Dil Nawaz Khan Marwat² · Jamilu Sabi'u³ · Mustafa Inc^{4,5,6}

Received: 24 September 2023 / Accepted: 5 December 2023 / Published online: 27 January 2024
© The Author(s) 2024

Abstract

In this paper, we present an innovative approach to acquire the exact solutions of the Shynaray-IIA equations (S-IIAE), by using the improved modified Sardar sub-equation method (IMSSEM). The S-IIAE are nonlinear and coupled partial differential equations that arise in various fields of physics and engineering such as optical fibers and ferromagnetic materials. The IMSSEM is applied to S-IIAE; we successfully derived exact solutions that accurately described the wave propagation behavior of the system under consideration. The obtained solutions include rational, trigonometric, and trigonometric hyperbolic function solutions. The obtained solutions are concise and offer a deeper insight into the dynamics and characteristics of the S-IIAE. Moreover, some of the new solutions to S-IIAE are plotted in different dimensions through which bright, anti-kink and bright solitary wave structures are established. The results of the study also indicated that the proposed method is a valuable approach for achieving analytical solutions to a wide range of nonlinear partial differential equations.

Keywords Optical soliton · Improved modified Sardar sub-equation method · Shynaray-IIA equation

✉ Mustafa Inc
minc@firat.edu.tr

Muhammad Ishfaq Khan
m.ishfaqkhan032@gmail.com

Dil Nawaz Khan Marwat
dnm512@yahoo.com

Jamilu Sabi'u
jsabiu@yumsuk.edu.ng

¹ Department of Mathematics, COMSATS University Islamabad, Islamabad, Pakistan

² Department of Mathematics, Faculty of Technologies and Engineering Sciences, Islamia College Peshawar, Jamrud Road University Campus, Peshawar 25120, Khyber Pakhtunkhwa, Pakistan

³ Department of Mathematics, Yusuf Maitama Sule University, Kano, Nigeria

⁴ Department of Mathematics, Firat University, 23119 Elazig, Turkey

⁵ Department of Computer Engineering, Biruni University, 34010 Istanbul, Turkey

⁶ Department of Medical Research, China Medical University, 40402 Taichung, Taiwan

1 Introduction

The nonlinear partial differential equations (NPDEs) are widely used for the representation of physical problems arising in various branches of science and engineering, and often they describe real phenomena of complex nature in physics, fluid dynamics, and many other fields. For example, the Korteweg and de Vries equation (1895), Fisher's equation (1951), the equation governing wave propagation in low-pass electrical transmission line (Houwe et al. 2020), the Biswas–Arshed equation (Sabi'u et al. 2019b), the Boussinesq-like equations (Shi et al. 2015; Mirhosseini-Alizamini et al. 2021), the incompressible Navier–Stokes equations in streamfunction-vorticity formulation (Raza et al. 2021), the Sine–Gordon equation (Ben-Yu et al. 1986), and the nonlinear Schrodinger equation (Kato 1987). The Shynaray-IIA Equation (S-IIAE) are coupled system of nonlinear PDEs, whereas, it involves significant challenges of a serious nature, which are associated with intricate and nontrivial behaviors of the system (Myrzakulova et al. 2022). The well-known mathematical form of S-IIAE (Fahim et al. 2022) is expressed below:

$$\begin{aligned}iq_t + q_{xt} - i(vq)_x &= 0, \\ir_t - r_{xt} - i(vr)_x &= 0, \\v_x - \frac{n^2}{m}(rq)_t &= 0,\end{aligned}\tag{1}$$

where $q(x, t)$, $r(x, t)$ and $v(x, t)$ represent the unknown variables and they naturally depend on independent variables x and t . Note that m and n are constants. The integrable property of this equation via the inverse scattering transform, other properties such as geometrical and gauge equivalence, and space curves integrable motion are extensively studied, see Sagidullayeva et al. (2022) and the reference therein.

The solution of NPDEs became a challenging problem in mathematics and engineering, especially to get the stability and consistency of such systems while finding numerical solutions (Shah et al. 2010; Hussain et al. 2019). The most commonly used numerical methods for solving the NPDE are the finite difference methods, spectral methods, finite element and finite volume methods (Ma and Yan 2006; Sod 1978; Fallah et al. 2000; Meuris et al. 2023). The non-numerical solutions of such equations are not an easy task all the time, therefore, the most serious concerns of researchers regarding the exact solutions to such equations have been addressed positively which is strictly based on the motivation of physical insights of the problem. The solitary wave methods are among the convincing methods for finding the exact solution to NPDEs. Previously, many methods have been used to find the exact solutions of NPDEs, such as the tanh method (Almatrafi 2023), the homogeneous balance method (Jafari et al. 2014), the sub-equation method (Akinoyemi et al. 2021; Senol et al. 2021), the Kudryashov method and its modifications (Kudryashov 2012, 2020), the sine-Gordon methods (Baskonus et al. 2019; Kumar et al. 2017a; Fahim et al. 2022), the generalized algebraic and Q -expansion methods (Almatrafi and Alharbi 2023; Alharbi and Almatrafi 2022), the Jacobi elliptic function expansion method (Khan et al. 2022), and so on, see Iqbal (2018), Bilal et al. (2021), Seadawy et al. (2021, 2019), Iqbal et al. (2023), Khatri et al. (2019), Kumar et al. (2017b, 2021), Dahiya et al. (2021), Sabi'u et al. (2019a, 2022, 2023) for more details and the references therein. In addition, some of the most accurate and efficient techniques were designed with extreme efforts of researchers for the solutions of NLPDEs. However, some of these methods do not provide reasonable solutions to the system of NLPDEs adequately. Therefore, this prompted us to apply IMSSEM (Akinoyemi 2021) for the solutions of S-IIAE. More precisely, the IMSSEM is a novel approach

that combines and utilizes the strengths of existing methodologies to offer robust and versatile solutions for nonlinear NPDEs.

The primary objective of this research paper is to present the exact solution to the challenging S-IIAE for the first time in the literature using the IMSSEM (Akinyemi 2021), by employing this innovative method, we aim to overcome the limitations of traditional approaches and provide concise and elegant solutions to this complex equation.

The structure of this work is as follows: we give a brief introduction to the importance of NPDEs in science and engineering and some available methods for solving them in Sect. 1. Section 2 contains the methodology of the suggested technique for the solution of S-IIAE. In Sect. 3, we used the IMSSEM to solve the S-IIAE precisely. Section 4 addresses the graphical depiction of the solutions. Section 5 of the study contains its conclusion.

2 Methodology of the proposed improved modified Sardar sub-equation method

This section will elucidate the procedures of the IMSSEM (Akinyemi 2021) for solving NPDEs. Now, Let us consider the NLPDE

$$F(u, u_t, u_x, u_{xx}, \dots) = 0, \tag{2}$$

where the function $u = u(x, t)$ represents an unknown function in the given context. In order to proceed, we have introduced a wave transformation as follows:

$$u = u(\eta) \text{ where } \eta = x - ct, \tag{3}$$

by using the transformation in Eq. (3) into the nonlinear PDE in Eq. (2), where $c \neq 0$, we can reduce the PDE into an ODE of integer order

$$N(u', u'', u''', \dots) = 0. \tag{4}$$

We have solved the ODE (4) by using the IMSSEM, the technique has the standard form:

$$u(\eta) = a_0 + \sum_{j=1}^N a_j \phi^j(\eta), \text{ where } a_N \neq 0, \tag{5}$$

where a_j ($j = 0, 1, 2, 3, \dots, N$).

The value of N can be determined by homogeneous balancing procedure (HBP), by balancing the highest order nonlinear and highest order derivative term in Eq. (4). Therefore, the highest degree of $\frac{d^r u}{d\eta^r}$ is classified as:

$$O\left(\frac{d^r u}{d\eta^r}\right) = n + r, \tag{6}$$

$$O\left(u^q \frac{d^r u}{d\eta^r}\right)^s = qn + s(n + r). \tag{7}$$

2.1 The enhanced improved modified Sardar sub-equation approach

The $\phi(\eta)$ in Eq. (5) is considered the solution to the following equation:

$$(\phi')^2(\eta) = \delta_2\phi^4(\eta) + \delta_1\phi^2(\eta) + \delta_0, \tag{8}$$

where $\delta_i, i = 0, 1, 2$ are constants to be determined, for more detail on Eq. (8) see Akinyemi (2021) and the references therein. The following set of solutions that satisfied Eq. (8) with C as the constant of integration are:

For $\delta_0 = \delta_1 = 0$ and $\delta_2 > 0$, we obtained the rational solutions:

$$\phi_1^\pm(\eta) = \pm \frac{1}{\sqrt{\delta_2}(\eta + C)}. \tag{9}$$

For $\delta_0 = 0$ and $\delta_1 > 0$, the exponential solutions will be of the form:

$$\phi_2^\pm(\eta) = \frac{4\delta_1 e^{\pm\sqrt{\delta_1}(\eta+C)}}{e^{\pm 2\sqrt{\delta_1}(\eta+C)} - 4\delta_1\delta_2}, \tag{10}$$

$$\phi_3^\pm(\eta) = \frac{\pm 4\delta_1 e^{\pm\sqrt{\delta_1}(\eta+C)}}{1 - 4\delta_1\delta_2 e^{\pm 2\sqrt{\delta_1}(\eta+C)}}. \tag{11}$$

The trigonometric hyperbolic solutions are as follows:

(i) For $\delta_0 = 0, \delta_1 > 0$ and $\delta_2 \neq 0$, we have

$$\phi_4^\pm(\eta) = \pm \sqrt{-\frac{\delta_1}{\delta_2}} \operatorname{sech}\left(\sqrt{\delta_1}(\eta + C)\right), \tag{12}$$

$$\phi_5^\pm(\eta) = \pm \sqrt{\frac{\delta_1}{\delta_2}} \operatorname{csch}\left(\sqrt{\delta_1}(\eta + C)\right). \tag{13}$$

(ii) For $\delta_0 = \frac{\delta_1^2}{4\delta_2}, \delta_1 < 0$ and $\delta_2 > 0$, we have

$$\phi_6^\pm(\eta) = \pm \sqrt{-\frac{\delta_1}{2\delta_2}} \tanh\left(\sqrt{-\frac{\delta_1}{2}}(\eta + C)\right), \tag{14}$$

$$\phi_7^\pm(\eta) = \pm \sqrt{-\frac{\delta_1}{2\delta_2}} \operatorname{coth}\left(\sqrt{-\frac{\delta_1}{2}}(\eta + C)\right), \tag{15}$$

$$\phi_8^\pm(\eta) = \pm \sqrt{-\frac{\delta_1}{2\delta_2}} \left(\tanh\left(\sqrt{-2\delta_1}(\eta + C)\right) \pm \operatorname{isech}\left(\sqrt{-2\delta_1}(\eta + C)\right)\right), \tag{16}$$

$$\phi_9^\pm(\eta) = \pm \sqrt{-\frac{\delta_1}{2\delta_2}} \left(\coth\left(\sqrt{-2\delta_1}(\eta + C)\right) \pm \operatorname{csch}\left(\sqrt{-2\delta_1}(\eta + C)\right) \right), \tag{17}$$

$$\phi_{10}(\eta) = \pm \sqrt{-\frac{\delta_1}{8\delta_2}} \left(\tanh\left(\sqrt{-\frac{\delta_1}{8}}(\eta + C)\right) + \coth\left(\sqrt{-\frac{\delta_1}{8}}(\eta + C)\right) \right). \tag{18}$$

The solutions which have the form of trigonometric functions are presented below:

(i) For $\delta_0 = 0$, $\delta_1 < 0$ and $\delta_2 \neq 0$, we have

$$\phi_{11}^\pm(\eta) = \pm \sqrt{-\frac{\delta_1}{\delta_2}} \sec\left(\sqrt{-\delta_1}(\eta + C)\right), \tag{19}$$

$$\phi_{12}^\pm(\eta) = \pm \sqrt{-\frac{\delta_1}{\delta_2}} \csc\left(\sqrt{-\delta_1}(\eta + C)\right). \tag{20}$$

(ii) For $\delta_0 = \frac{\delta_1^2}{4\delta_2}$, $\delta_1 > 0$ and $\delta_2 > 0$, we have

$$\phi_{13}^\pm(\eta) = \pm \sqrt{\frac{\delta_1}{2\delta_2}} \tan\left(\sqrt{\frac{\delta_1}{2}}(\eta + C)\right), \tag{21}$$

$$\phi_{14}^\pm(\eta) = \pm \sqrt{\frac{\delta_1}{2\delta_2}} \cot\left(\sqrt{\frac{\delta_1}{2}}(\eta + C)\right), \tag{22}$$

$$\phi_{15}^\pm(\eta) = \pm \sqrt{\frac{\delta_1}{2\delta_2}} \left(\tan\left(\sqrt{2\delta_1}(\eta + C)\right) \pm \sec\left(\sqrt{2\delta_1}(\eta + C)\right) \right), \tag{23}$$

$$\phi_{16}^\pm(\eta) = \pm \sqrt{\frac{\delta_1}{2\delta_2}} \left(\cot\left(\sqrt{2\delta_1}(\eta + C)\right) \pm \csc\left(\sqrt{2\delta_1}(\eta + C)\right) \right), \tag{24}$$

$$\phi_{17}^\pm(\eta) = \pm \sqrt{\frac{\delta_1}{8\delta_2}} \left(\tan\left(\sqrt{\frac{\delta_1}{8}}(\eta + C)\right) - \cot\left(\sqrt{\frac{\delta_1}{8}}(\eta + C)\right) \right). \tag{25}$$

Remember that we have substituted Eqs. (5 and 8) into Eq. (4), and equate all the coefficients of each power of $\phi(\eta)$ to zero and solve the resultant system of algebraic equations with the help of Maple. Eventually, we incorporated these constants (coefficients) into Eq. (5) and obtained the solution of distinct types as shown in Eqs. (9–25). As a result, we obtained different exact solutions for NPDEs.

3 Shynaray-IIA equation (S-IIAE) and its solutions by Sardar sub-equation method

In this section, we present the exact solutions of S-IIAE (1) by IMSSEM (Akinyemi 2021)

$$\begin{aligned} iq_t + q_{xt} - i(vq)_x &= 0, \\ ir_t - r_{xt} - i(vr)_x &= 0, \\ v_x - \frac{n^2}{m}(rq)_t &= 0. \end{aligned}$$

In case when $r = \epsilon \bar{q}$ ($\epsilon = \pm 1$), the S-IIAE takes the following form

$$\begin{aligned} iq_t + q_{xt} - i(vq)_x &= 0, \\ v_x - \frac{n^2}{m}(|q|^2)_t &= 0. \end{aligned} \tag{26}$$

In the above equation m, n and ϵ are constants. By using the traveling wave transformation, Eq. (26) is reduced into the following ODE

$$\begin{aligned} q(x, t) &= U(\eta)e^{i\xi(x,t)}, v(x, t) = G(\eta), \\ \xi(x, t) &= -\delta x + \omega t + \theta, \eta = x - ct, \end{aligned} \tag{27}$$

where $v, \theta, \omega, \delta$ characterize the frequency, phase constant, wave number and velocity of soliton, respectively. Substituting Eq. (27) into the first part of the system (26) and separating the real and imaginary parts, we have the real part of the form

$$\begin{aligned} cU''(\eta) + \omega(1 - \delta)U(\eta) + \delta G(\eta)U(\eta) + i(\omega - c(1 - \delta))U'(\eta) - G(\eta)U'(\eta) - G'(\eta)U(\eta) &= 0, \\ G'(\eta) + \frac{2cn^2}{m}U(\eta)U'(\eta) &= 0. \end{aligned} \tag{28}$$

Equation (28) is integrated, and we get

$$G(\eta) = -\frac{cen^2}{m}U^2(\eta). \tag{29}$$

Substitute Eq. (29) into the first part of (28) and separate the real and imaginary parts as

$$cU''(\eta) + \omega(1 - \delta)U(\eta) - \frac{\delta cen^2}{m}U^3(\eta) = 0, \tag{30}$$

where the imaginary part is given by

$$(\omega - c(1 - \delta))U'(\eta) + \frac{3cen^2}{m}U''(\eta)U'(\eta) = 0. \tag{31}$$

By using the HBP, by balancing the highest order derivative and highest order nonlinear term, we obtained $N = 1$. The determined value of N is substituted in Eq. (5), we obtain the simple form of the solution as:

$$U(\eta) = a_0 + a_1\phi(\eta). \tag{32}$$

3.1 Exact solutions of S-IIAE by IMSSEM

In this section, Eqs. (8 and 32) are substituted into Eq. (30) and we get the following equation with the aid of Maple.

$$\begin{aligned} &\frac{1}{m}(\omega ma_0 + \omega ma_1 U(\eta) - \omega n\delta a_0 - \omega m\delta a_1 U(\eta) - \delta cn^2 a_0^3 \\ &\quad - 3\delta cn^2 a_0^2 a_1^2 U(\eta) - 3\delta cn^2 a_0 a_1^2 U^2(\eta) - \delta cn^2 a_1^3 U^3(\eta) \\ &\quad + 2ca_1 U^3(\eta)m\delta_2 + ca_1 U(\eta)m\delta_1 = 0. \end{aligned} \tag{33}$$

By comparing the coefficients of various powers of $U^i(\eta)$, we get the system of algebraic equations of the following form, we have

$$U^0 : \frac{-a_0(-\omega m + \omega m\delta + \delta\epsilon cn^2 b_0^2)}{m} = 0, \tag{34}$$

$$U^1 : \frac{\omega ma_1 - \omega m\delta a_1 - 3\delta\epsilon cn^2 a_0^2 a_1 + ca_1 m\delta_1}{m} = 0, \tag{35}$$

$$U^2 : \frac{-3\delta\epsilon cn^2 a_0 a_1^2}{m} = 0, \tag{36}$$

$$U^3 : \frac{-\delta\epsilon cn^2 a_1^3 + 2ca_1 m\delta_2}{m} = 0. \tag{37}$$

Solving the above system of equations with the aid of Maple and get the coefficients:

$$a_0 = 0, \tag{38}$$

$$a_1 = a_1, \tag{39}$$

$$\delta_1 = \frac{\omega(-1 + \delta)}{c}, \tag{40}$$

$$\delta_2 = \frac{\delta\epsilon n^2 a_1^2}{2m}. \tag{41}$$

Using Eqs. (39–41) in combination with Eqs. (9–25) and Eq. (32), we obtained the following solutions.

The rational solution of Eq. (1) for $\delta_0 = \delta_1 = 0$ and $\delta_2 > 0$ can be found as:

$$U_1^\pm(\eta) = \pm \frac{1}{\sqrt{\delta_2}(\eta + C)}. \tag{42}$$

The exponential solutions of Eq. (1) have the following form:

For $\delta_0 = 0$ and $\delta_1 > 0$, we have

$$U_2^\pm(\eta) = \frac{4 \frac{\omega(-1+\delta)}{c} e^{\pm \sqrt{\frac{\omega(-1+\delta)}{c}}(\eta+C)}}{e^{\pm 2 \sqrt{\frac{\omega(-1+\delta)}{c}}(\eta+C)} - 2 \frac{\omega(-1+\delta)\delta\epsilon n^2 a_1^2}{cm}}, \tag{43}$$

$$U_3^\pm(\eta) = \frac{\pm 4 \frac{\omega(-1+\delta)}{c} e^{\pm \sqrt{\frac{\omega(-1+\delta)}{c}}(\eta+C)}}{1 - 2 \frac{\omega(-1+\delta)\delta\epsilon n^2 a_1^2}{cm} e^{\pm 2 \sqrt{\frac{\omega(-1+\delta)}{c}}(\eta+C)}}. \tag{44}$$

The trigonometric and hyperbolic solutions of Eq. (1) are given as:

For $\delta_0 = 0, \delta_1 > 0$ and $\delta_2 \neq 0$, we have

$$U_4^\pm(\eta) = \pm \sqrt{-\frac{2m\omega(-1+\delta)}{c\delta\epsilon n^2 a_1^2}} \operatorname{sech}\left(\sqrt{\frac{\omega(-1+\delta)}{c}}(\eta+C)\right), \tag{45}$$

$$U_5^\pm(\eta) = \pm \sqrt{\frac{2m\omega(-1+\delta)}{c\delta\epsilon n^2 a_1^2}} \operatorname{csch}\left(\sqrt{\frac{\omega(-1+\delta)}{c}}(\eta+C)\right). \tag{46}$$

- While for $\delta_0 = \frac{\delta_1^2}{4\delta^2}, \delta_1 < 0$ and $\delta_2 > 0$, we get the solutions as:

$$U_6^\pm(\eta) = \pm \sqrt{-\frac{m\omega(-1+\delta)}{c\delta\epsilon n^2 a_1^2}} \tanh\left(\sqrt{-\frac{\omega(-1+\delta)}{2c}}(\eta+C)\right), \tag{47}$$

$$U_7^\pm(\eta) = \pm \sqrt{-\frac{m\omega(-1+\delta)}{c\delta\epsilon n^2 a_1^2}} \operatorname{coth}\left(\sqrt{-\frac{\omega(-1+\delta)}{2c}}(\eta+C)\right), \tag{48}$$

$$U_8^\pm(\eta) = \pm \sqrt{-\frac{m\omega(-1+\delta)}{c\delta\epsilon n^2 a_1^2}} (\tanh\left(\sqrt{-2\frac{\omega(-1+\delta)}{c}}(\eta+C)\right) \pm \operatorname{isch}\left(\sqrt{-2\frac{\omega(-1+\delta)}{c}}(\eta+C)\right)), \tag{49}$$

$$U_9^\pm(\eta) = \pm \sqrt{-\frac{m\omega(-1+\delta)}{c\delta\epsilon n^2 a_1^2}} (\operatorname{coth}\left(\sqrt{-2\frac{\omega(-1+\delta)}{c}}(\eta+C)\right) \pm \operatorname{csch}\left(\sqrt{-2\frac{\omega(-1+\delta)}{c}}(\eta+C)\right)), \tag{50}$$

$$U_{10}(\eta) = \pm \sqrt{-\frac{m\omega(-1+\delta)}{4c\delta\epsilon n^2 a_1^2}} (\tanh\left(\sqrt{-\frac{\omega(-1+\delta)}{8c}}(\eta+C)\right) + \operatorname{coth}\left(\sqrt{-\frac{\omega(-1+\delta)}{8c}}(\eta+C)\right)). \tag{51}$$

- The trigonometric solutions of Eq. (1) are stated as:

(i) For $\delta_0 = 0, \delta_1 < 0, \delta_2 \neq 0$ and $\delta < 1$, we have

$$U_{11}^\pm(\eta) = \pm \sqrt{-\frac{2m\omega(-1+\delta)}{c\delta\epsilon n^2 a_1^2}} \operatorname{sec}\left(\sqrt{-\frac{\omega(-1+\delta)}{c}}(\eta+C)\right), \tag{52}$$

$$U_{12}^{\pm}(\eta) = \pm \sqrt{-\frac{2m\omega(-1 + \delta)}{c\delta\epsilon n^2 a_1^2}} \operatorname{csc}\left(\sqrt{-\frac{\omega(-1 + \delta)}{c}}(\eta + C)\right), \tag{53}$$

(ii) For $\delta_0 = \frac{\delta_1^2}{4\delta_2}$, $\delta_1 > 0$, $\delta_2 > 0$ and $\delta > 1$, we have

$$U_{13}^{\pm}(\eta) = \pm \sqrt{\frac{m\omega(-1 + \delta)}{c\delta\epsilon n^2 a_1^2}} \tan\left(\sqrt{\frac{\omega(-1 + \delta)}{2c}}(\eta + C)\right), \tag{54}$$

$$U_{14}^{\pm}(\eta) = \pm \sqrt{\frac{m\omega(-1 + \delta)}{c\delta\epsilon n^2 a_1^2}} \cot\left(\sqrt{\frac{\omega(-1 + \delta)}{2c}}(\eta + C)\right), \tag{55}$$

$$U_{15}^{\pm}(\eta) = \pm \sqrt{\frac{m\omega(-1 + \delta)}{c\delta\epsilon n^2 a_1^2}} \left(\tan\left(\sqrt{2\frac{\omega(-1 + \delta)}{c}}(\eta + C)\right) \pm \sec\left(\sqrt{2\frac{\omega(-1 + \delta)}{c}}(\eta + C)\right)\right), \tag{56}$$

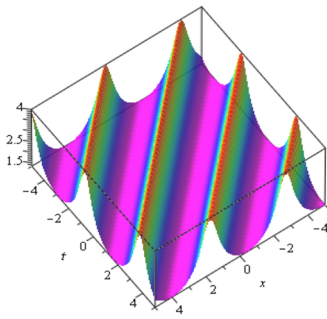
$$U_{16}^{\pm}(\eta) = \pm \sqrt{\frac{m\omega(-1 + \delta)}{c\delta\epsilon n^2 a_1^2}} \left(\cot\left(\sqrt{2\frac{\omega(-1 + \delta)}{c}}(\eta + C)\right) \pm \operatorname{csc}\left(\sqrt{2\frac{\omega(-1 + \delta)}{c}}(\eta + C)\right)\right), \tag{57}$$

$$U_{17}^{\pm}(\eta) = \pm \sqrt{\frac{m\omega(-1 + \delta)}{4c\delta\epsilon n^2 a_1^2}} \left(\tan\left(\sqrt{\frac{\omega(-1 + \delta)}{8c}}(\eta + C)\right) - \cot\left(\sqrt{\frac{\omega(-1 + \delta)}{8c}}(\eta + C)\right)\right). \tag{58}$$

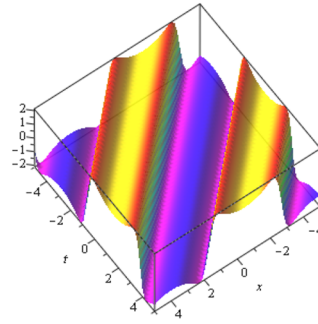
Therefore, the corresponding solution to Eq. (26) can be obtained by using the transformations $q(x, t) = U(\eta)e^{i\xi(x,t)}$, $v(x, t) = G(\eta)$, $r = \epsilon\bar{q}$ ($\epsilon = \pm 1$), with $G(\eta) = -\frac{c\epsilon n^2}{m}U^2(\eta)$.

4 The results and discussions

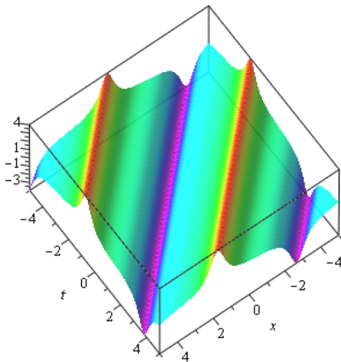
This section provides the result discussions on the derived solutions for the system of S-IIAE using IMSSEM. The derived solutions are rational, exponential, trigonometric and hyperbolic function solutions. for example, the solution Eq. (42) is a rational function solution, Eqs. (43) and (44) correspond to the exponential function solutions, Eqs. (45) to (51) represent the hyperbolic function solutions, and Eqs. (52) to (58) are trigonometric functions solutions. Moreover, Fig. 1 gives the graphical representations for some of the derived solitary wave solutions to Fig. 6. All the shapes in Figs. 1, 2, 3, 4, 5 and 6 are recovered using $\epsilon = 1, \delta = -0.5, \omega = 1, a = 0, \eta = 1, a_1 = 2, c = 1, k = 1, C = 1, y = 0$, and $m = 1$. Moreover, all the 2D plots are recovered at $t = 0.2$. It is important to note that for the sake of demonstration of some of the solitary wave structures in Figs. 1, 2, 3, 4, 5 and 6, we plotted the solutions $U(\eta)$ and $G(\eta)$ from the derived solutions Eqs. (42) to (58). Among the important recovered structure are the dark, bright, kink and multiple wave



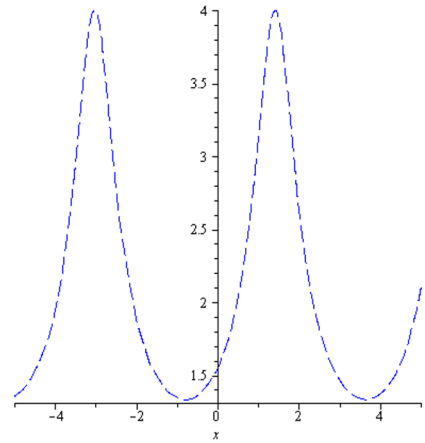
a. The 3D plot for $|U_2^\pm(\eta)|$.



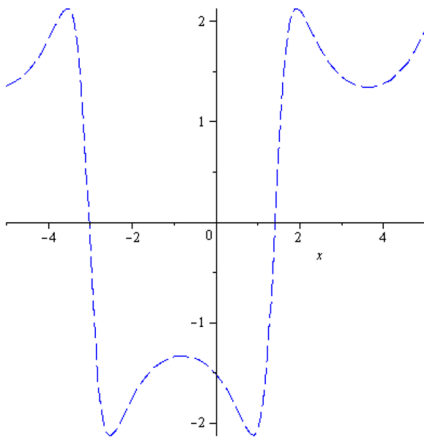
b. The 3D plot for the Real part of $U_2^\pm(\eta)$.



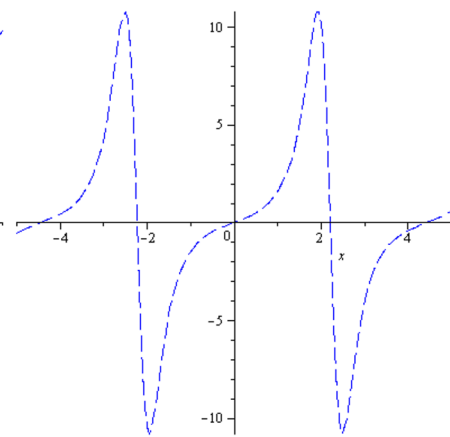
c. The 3D plot for the imaginary part of $U_2^\pm(\eta)$.



d. The 2D plot of $|U_2^\pm(\eta)|$.

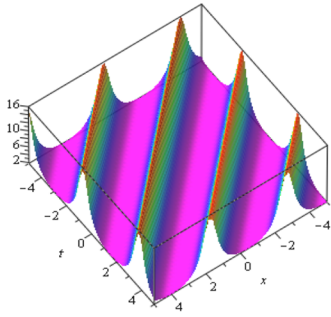


e. The 2D plot for the Real part of $U_2^\pm(\eta)$.

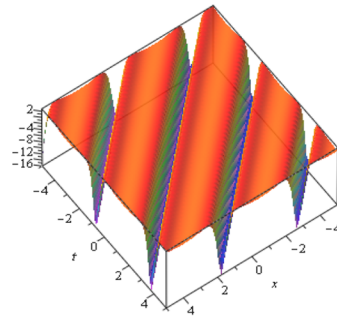


f. The 2D plot for the Real part of $U_2^\pm(\eta)$.

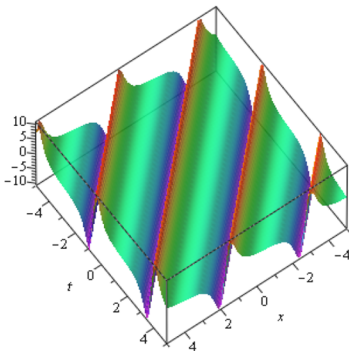
Fig. 1 The multiple soliton waves in 3D and 2D plots for the absolute, real and imaginary parts of $U_2^\pm(\eta)$.



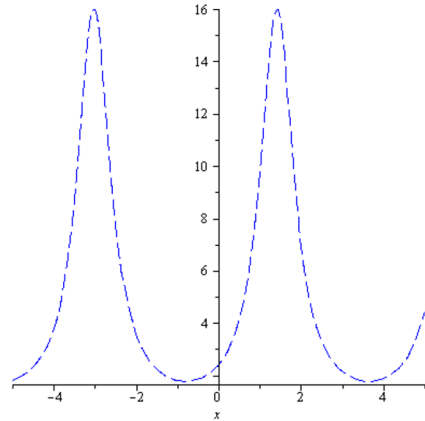
a. The 3D plot for $|G_2^\pm(\eta)|$.



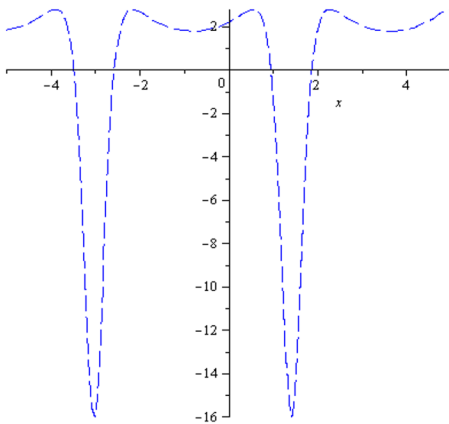
b. The 3D plot for the Real part of $G_2^\pm(\eta)$.



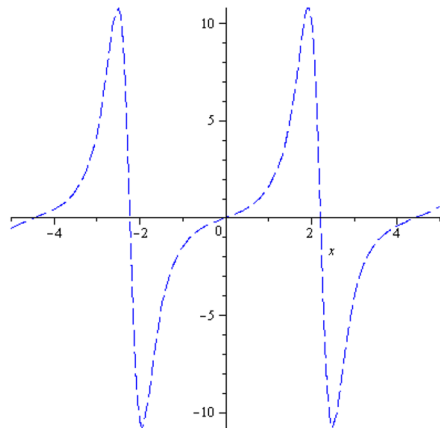
c. The 3D plot for the imaginary part of $G_2^\pm(\eta)$.



d. The 2D plot of $|G_2^\pm(\eta)|$.

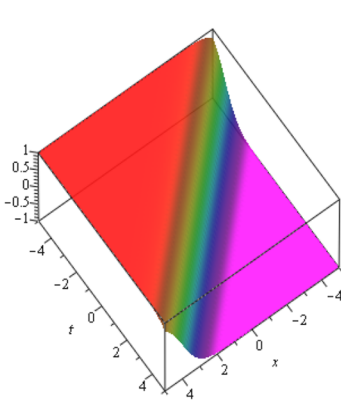


e. The 2D plot for the Real part of $G_2^\pm(\eta)$.

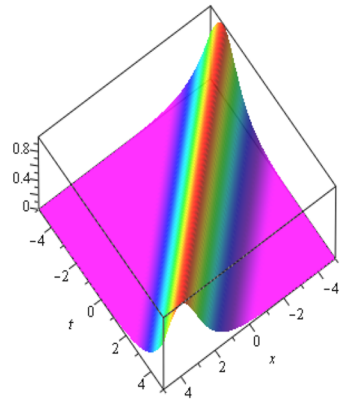


f. The 2D plot for the imaginary part of $G_2^\pm(\eta)$.

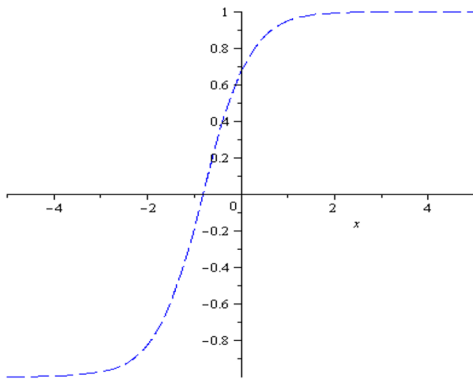
Fig. 2 The multiple soliton waves in 3D and 2D plots for the absolute, real and imaginary parts of $G_2^\pm(\eta)$.



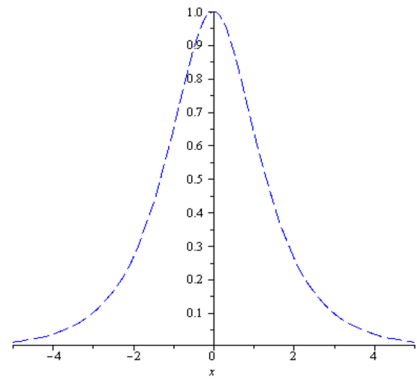
a. The 3D plot for the Real part of $U_{10}^{\pm}(\eta)$.



b. The 3D plot for the imaginary part of $U_{10}^{\pm}(\eta)$.



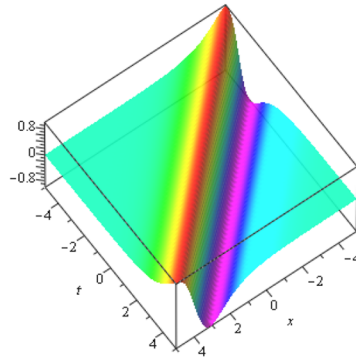
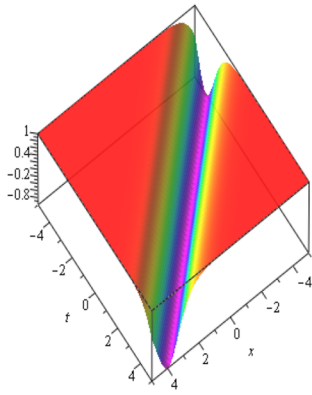
c. The 2D plot for the Real part of $U_{10}^{\pm}(\eta)$.



d. The 2D plot for the imaginary part of $U_{10}^{\pm}(\eta)$.

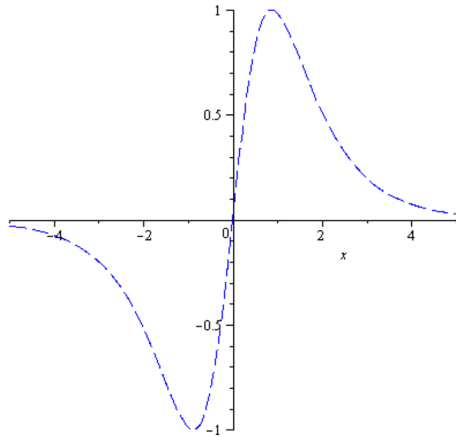
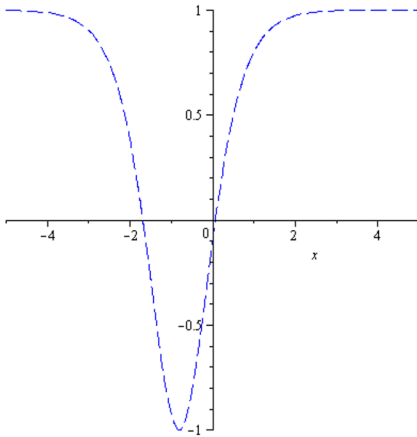
Fig. 3 **a** The kink soliton and **b** bright soliton in 3D and 2D plots for the absolute, real and imaginary parts of $U_{10}^{\pm}(\eta)$.

solitons. For example, Figs. 1, 2, 5b and 6b give the multiple wave solitons, Figs. 3a and 5a represent the kink soliton waves. Figures 3b and 5b represent the bright soliton whereas Figs. 4a and 6a represent the dark solitons.



a. The 3D plot for the Real part of $G_{10}^{\pm}(\eta)$.

b. The 3D plot for the imaginary part of $G_{10}^{\pm}(\eta)$.



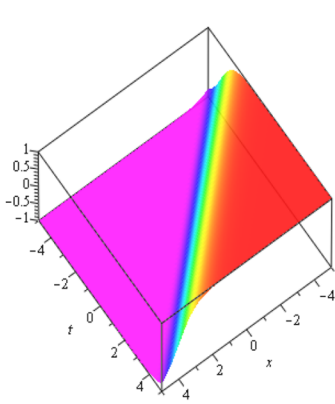
c. The 2D plot for the Real part of $G_{10}^{\pm}(\eta)$.

d. The 2D plot for the imaginary part of $G_{10}^{\pm}(\eta)$.

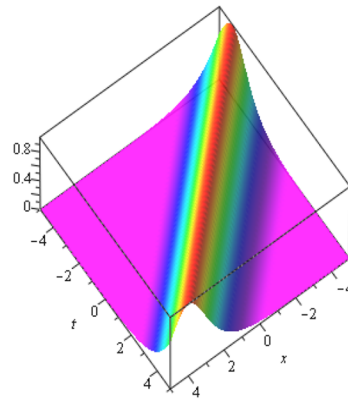
Fig. 4 **a** The dark soliton, and **b** multiple wave soliton in 3D and 2D plots for the absolute, real and imaginary parts of $G_{10}^{\pm}(\eta)$.

5 Conclusion

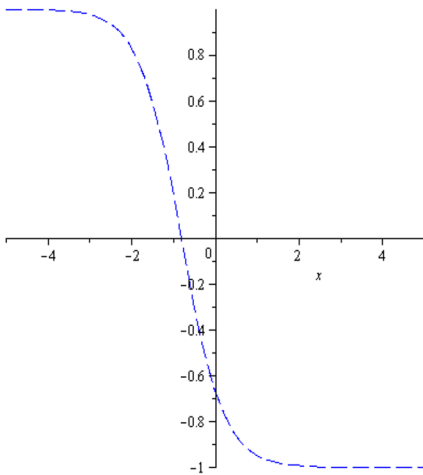
In this research paper, we presented a novel approach especially for obtaining the exact solutions to the S-IIAE, by employing the IMSSEM. The study successfully derived a family of exact solutions for these equations. These solutions provide valuable insights into the dynamics and behavior of S-IIAE and can be utilized in various fields of physics, and applied mathematics. The behavior of the solutions for the direct study is presented in two and three-dimensional graphs. The proposed technique offers a promising avenue for tackling other complex nonlinear equations and warrants further exploration in future research. Future studies of S-IIAE can be considered on the analytical, semi-analytical and



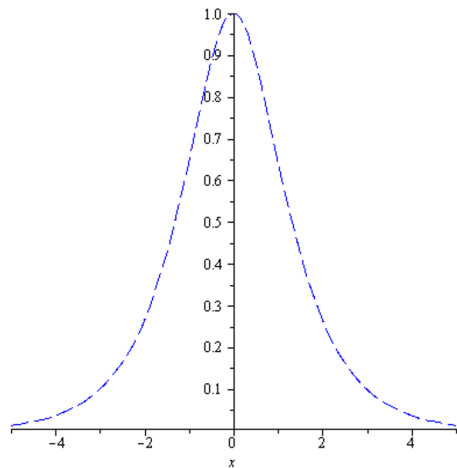
a. The 3D plot for the real part of $U_{15}^{\pm}(\eta)$.



b. The 3D plot for the imaginary part of $U_{15}^{\pm}(\eta)$.



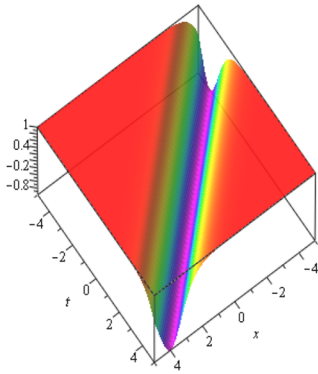
c. The 2D plot for the real part of $U_{15}^{\pm}(\eta)$.



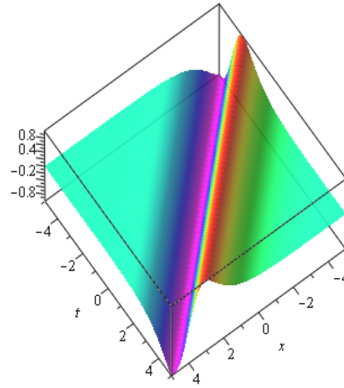
d. The 2D plot for the imaginary part of $U_{15}^{\pm}(\eta)$.

Fig. 5 **a** The anti-kink soliton and **b** bright soliton 3D and 2D plots for the absolute, real and imaginary parts of $U_{15}^{\pm}(\eta)$.

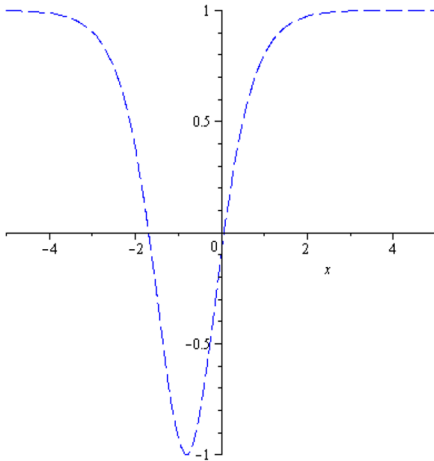
numerical solutions to investigate a variety of interesting results related to the indicated model, including the modulation instability and consistency of the solutions, their physical feasibility, and lie symmetry analysis.



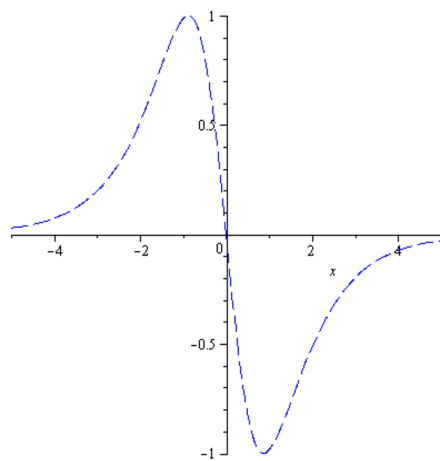
a. The 3D plot for the real part of $G_{15}^{\pm}(\eta)$.



c. The 3D plot for the imaginary part of $G_{15}^{\pm}(\eta)$.



c. The 2D plot for the real part of $G_{15}^{\pm}(\eta)$.



d. The 2D plot for the imaginary part of $G_{15}^{\pm}(\eta)$.

Fig. 6 **a** The dark soliton, and **b** multiple wave soliton in 3D and 2D plots for the absolute, real and imaginary parts of $G_{15}^{\pm}(\eta)$.

Author contributions Conceptualization; Methodology: [MIK]; Formal analysis and investigation: [DNKM]; Writing—original draft preparation: [JS]; Writing—review and editing: [MI].

Funding Open access funding provided by the Scientific and Technological Research Council of Türkiye (TÜBİTAK).

Data availability Data sharing does not apply to this article as no datasets were generated or analyzed during this study.

Declarations

Conflict of interest The authors declare that they have no conflict of interest.

Ethics approval Not applicable.

Consent for publication All the authors have agreed and given their consent for the publication of this research paper.

Open Access This article is licensed under a Creative Commons Attribution 4.0 International License, which permits use, sharing, adaptation, distribution and reproduction in any medium or format, as long as you give appropriate credit to the original author(s) and the source, provide a link to the Creative Commons licence, and indicate if changes were made. The images or other third party material in this article are included in the article's Creative Commons licence, unless indicated otherwise in a credit line to the material. If material is not included in the article's Creative Commons licence and your intended use is not permitted by statutory regulation or exceeds the permitted use, you will need to obtain permission directly from the copyright holder. To view a copy of this licence, visit <http://creativecommons.org/licenses/by/4.0/>.

References

- Akinyemi, L.: Two improved techniques for the perturbed nonlinear Biswas–Milovic equation and its optical solitons. *Optik* **243**, 167477 (2021)
- Akinyemi, L., Şenol, M., Iyiola, O.S.: Exact solutions of the generalized multidimensional mathematical physics models via sub-equation method. *Math. Comput. Simul* **182**, 211–233 (2021)
- Alharbi, A.R., Almatrafi, M.B.: Exact solitary wave and numerical solutions for geophysical KdV equation. *J. King Saud Univ. Sci.* **34**(6), 102087 (2022)
- Almatrafi, M.B.: Solitary wave solutions to a fractional model using the improved modified extended tanh-function method. *Fractal Fract.* **7**(3), 252 (2023)
- Almatrafi, M.B., Alharbi, A.: New soliton wave solutions to a nonlinear equation arising in plasma physics. *CMES-Comput. Model. Eng. Sci.* **137**(1), 827–841 (2023)
- Baskonus, H.M., Bulut, H., Sulaiman, T.A.: New complex hyperbolic structures to the Lonngren-wave equation by using sine-Gordon expansion method. *Appl. Math. Nonlinear Sci.* **4**(1), 129–138 (2019)
- Ben-Yu, G., Pascual, P.J., Rodriguez, M.J., Vázquez, L.: Numerical solution of the sine-Gordon equation. *Appl. Math. Comput.* **18**(1), 1–14 (1986)
- Bilal, M., Seadawy, A.R., Younis, M., Rizvi, S.T.R., El-Rashidy, K., Mahmoud, S.F.: Analytical wave structures in plasma physics modelled by Gilson–Pickering equation by two integration norms. *Results Phys.* **23**, 103959 (2021)
- Dahiya, S., Kumar, H., Kumar, A., Gautam, M.S.: Optical solitons in twin-core couplers with the nearest neighbor coupling. *Partial Differ. Equ. Appl. Math.* **4**, 100136 (2021)
- Fahim, M.R.A., Kundu, P.R., Islam, M.E., Akbar, M.A., Osman, M.S.: Wave profile analysis of a couple of (3+1)-dimensional nonlinear evolution equations by sine-Gordon expansion approach. *J. Ocean Eng. Sci.* **7**(3), 272–279 (2022)
- Fallah, N.A., Bailey, C., Cross, M., Taylor, G.A.: Comparison of finite element and finite volume methods application in geometrically nonlinear stress analysis. *Appl. Math. Model.* **24**(7), 439–455 (2000)
- Fisher, J.C.: Calculation of diffusion penetration curves for surface and grain boundary diffusion. *J. Appl. Phys.* **22**(1), 74–77 (1951)
- Houwe, A., Sabi'u, J., Hammouch, Z., Doka, S.Y.: Solitary pulses of a conformable nonlinear differential equation governing wave propagation in low-pass electrical transmission line. *Phys. Scr.* **95**(4), 045203 (2020)
- Hussain, S., Shah, A., Ayub, S., Ullah, A.: An approximate analytical solution of the Allen–Cahn equation using homotopy perturbation method and homotopy analysis method. *Heliyon* **5**(12), e03060 (2019)
- Iqbal, M., Seadawy, A.R., Lu, D.: Construction of solitary wave solutions to the nonlinear modified Korteweg–de Vries dynamical equation in unmagnetized plasma via mathematical methods. *Mod. Phys. Lett. A* **33**, 32–85 (2018)
- Iqbal, M., Seadawy, A.R., Lu, D., Zhang, Z.: Structure of analytical and symbolic computational approach of multiple solitary wave solutions for nonlinear Zakharov–Kuznetsov modified equal width equation. *Numer. Methods Partial Differ. Equ.* (2023)
- Jafari, H., Tajadodi, H., Baleanu, D.: Application of a homogeneous balance method to exact solutions of nonlinear fractional evolution equations. *J. Comput. Nonlinear Dyn.* **9**(2), 021019 (2014)
- Kato, T.: On nonlinear Schrödinger equations. *Annales De l'IHP Physique Théorique* **46**(1), 113–129 (1987)
- Khan, M.I., Asghar, S., Sabi'u, J.: Jacobi elliptic function expansion method for the improved modified Korteweg–de Vries equation. *Opt. Quant. Electron.* **54**(11), 734 (2022)

- Khatri, H., Gautam, M.S., Malik, A.: Localized and complex soliton solutions to the integrable (4+1)-dimensional Fokas equation. *SN Appl. Sci.* **1**, 1–9 (2019)
- Korteweg, D.J., De Vries, G.: XLI. On the change of form of long waves advancing in a rectangular canal, and on a new type of long stationary waves. *Lond. Edinb. Dublin Philos. Mag. J. Sci.* **39**(240), 422–443 (1895)
- Kudryashov, N.A.: One method for finding exact solutions of nonlinear differential equations. *Commun. Nonlinear Sci. Numer. Simul.* **17**(6), 2248–2253 (2012)
- Kudryashov, N.A.: Method for finding highly dispersive optical solitons of nonlinear differential equations. *Optik* **206**, 163550 (2020)
- Kumar, D., Hosseini, K., Samadani, F.: The sine-Gordon expansion method to look for the traveling wave solutions of the Tzitzéica type equations in nonlinear optics. *Optik* **149**, 439–446 (2017a)
- Kumar, H., Malik, A., Singh Gautam, M., Chand, F.: Dynamics of shallow water waves with various Boussinesq equations. *Acta Phys. Pol. A* **131**(2), 275–282 (2017b)
- Kumar, H., Kumar, A., Chand, F., Singh, R.M., Gautam, M.S.: Construction of new traveling and solitary wave solutions of a nonlinear PDE characterizing the nonlinear low-pass electrical transmission lines. *Phys. Scr.* **96**(8), 085215 (2021)
- Ma, Q.W., Yan, S.: Quasi ALE finite element method for nonlinear water waves. *J. Comput. Phys.* **212**(1), 52–72 (2006)
- Meuris, B., Qadeer, S., Stinis, P.: Machine-learning-based spectral methods for partial differential equations. *Sci. Rep.* **13**(1), 1739 (2023)
- Mirhosseini-Alizamini, S.M., Ullah, N., Sabi'u, J., Rezazadeh Inc, H.M.: New exact solutions for nonlinear Atangana conformable Boussinesq-like equations by new Kudryashov method. *Int. J. Mod. Phys. B* **35**(12), 2150163 (2021)
- Myrzakulova, Z., Nugmanova, G., Yesmakhanova, K., Myrzakulov, R.: Integrable motion of anisotropic space curves and surfaces induced by the Landau–Lifshitz equation. *arXiv preprint arXiv:2202.00748* (2022).
- Raza, S., Rauf, A., Sabi'u, J., Shah, A.: A numerical method for solution of incompressible Navier–Stokes equations in streamfunction–vorticity formulation. *Comput. Math. Methods* **3**(6), e1188 (2021)
- Sabi'u, J., Jibril, A., Gadu, A.M.: New exact solution for the (3+ 1) conformable space–time fractional modified Korteweg–de Vries equations via Sine-Cosine Method. *J. Taibah Univ. Sci.* **13**(1), 91–95 (2019a)
- Sabi'u, J., Rezazadeh, H., Tariq, H., Bekir, A.: Optical solitons for the two forms of Biswas–Arshed equation. *Mod. Phys. Lett. B* **33**(25), 1950308 (2019b)
- Sabiu, J., Rezazadeh, H., Cimpoiasu, R., Constantinescu, R.: Traveling wave solutions of the generalized Rosenau–Kawahara-RLW equation via the sine–cosine method and a generalized auxiliary equation method. *Int. J. Nonlinear Sci. Numer. Simul.* **23**(3–4), 539–551 (2022)
- Sabi'u, J., Inc, M., Leta, T.D., Baleanu, D., Rezazadeh, H.: Dynamical behaviour of the Joseph–Egri equation. *Therm. Sci.* **27**(1), 19–28 (2023)
- Sagidullayeva, Z., Yesmakhanova, K., Serikbayev, N., Nugmanova, G., Yerzhanov, K., Myrzakulov, R.: Integrable generalized Heisenberg ferromagnet equations in 1+1 dimensions: reductions and gauge equivalence. *arXiv:2205.02073*
- Seadawy, A.R., Iqbal, M., Lu, D.: Applications of propagation of long-wave with dissipation and dispersion in nonlinear media via solitary wave solutions of generalized Kadomtsev–Petviashvili modified equal width dynamical equation. *Comput. Math. Appl.* **78**(11), 3620–3632 (2019)
- Seadawy, A.R., Iqbal, M., Althobaiti, S., Sayed, S.: Wave propagation for the nonlinear modified Korteweg–de Vries Zakharov–Kuznetsov and extended Zakharov–Kuznetsov dynamical equations arising in nonlinear wave media. *Opt. Quant. Electron.* **53**, 1–20 (2021)
- Senol, M., Akinyemi, L., Ata, A., Iyiola, O.S.: Approximate and generalized solutions of conformable type Coudrey–Dodd–Gibbon–Sawada–Kotera equation. *Int. J. Mod. Phys. B* **35**(02), 2150021 (2021)
- Shah, A., Yuan, L., Khan, A.: Upwind compact finite difference scheme for time-accurate solution of the incompressible Navier–Stokes equations. *Appl. Math. Comput.* **215**(9), 3201–3213 (2010)
- Shi, C.G., Zhao, B.Z., Ma, W.X.: Exact rational solutions to a Boussinesq-like equation in (1+1)-dimensions. *Appl. Math. Lett.* **48**, 170–176 (2015)
- Sod, G.A.: A survey of several finite difference methods for systems of nonlinear hyperbolic conservation laws. *J. Comput. Phys.* **27**(1), 1–31 (1978)